Testing Bell inequality through $h\to\tau\tau$ at CEPC*

Kai Ma (马凯)[1†] Tong Li (李佟)[2‡]

[1]Faculty of Science, Xi'an University of Architecture and Technology, Xi'an 710055, China
[2]School of Physics, Nankai University, Tianjin 300071, China

Abstract: The decay of Higgs boson into two spin-1/2 particles provides an ideal system to reveal quantum entanglement and Bell-nonlocality. Future e^+e^- colliders can improve the measurement accuracy of the spin correlation of tau lepton pairs from Higgs boson decay. We show the testability of Bell inequality through $h\to\tau\tau$ at Circular Electron Positron Collider (CEPC). Two realistic methods of testing Bell inequality are investigated, *i.e.*, Törnqvist's method and Clauser-Home-Shimony-Holt (CHSH) inequality. In the simulation, we consider the detector effects of CEPC including uncertainties for tracks and jets from Z boson in the production of $e^+e^-\to Zh$. Necessary reconstruction approaches are described to measure quantum entanglement between τ^+ and τ^-. Finally, we show the sensitivity of CEPC to Bell inequality violation for the two methods.

Keywords: Bell inequality, Higgs boson, CEPC

DOI: 10.1088/1674-1137/ad62d8

I. INTRODUCTION

It is well known that the most significant debate regarding whether Quantum Mechanics (QM) is a complete local theory stems from the challenge raised by Einstein, Podolsky, and Rosen, commonly known as the EPR paradox [1]. The interpretation of the EPR paradox in local hidden variable theory (LHVT) shows the contradiction of LHVT with QM and presents the non-local nature of QM. Subsequently, Bohm et al. proposed a realistic experiment with a system of two spin-1/2 particles to illustrate the EPR paradox [2]. Based on this consideration, Bell established a theorem that the two particles' spin correlation satisfies a Bell inequality (BI) in realistic LHVT [3]. By contrast, the QM predictions may violate this inequality in some certain parameter space. Furthermore, Clauser, Horne, Shimony, and Holt (CHSH) generalized the original Bell inequality and established a more practical inequality [4]. The test of the Bell inequality delivers a direct justification if the QM is a complete local theory [5].

In the past, the violation of this Bell inequality has been observed in many low-energy experiments (such as optical experiments) [6−13] as the foundation of modern quantum information theory. The predictions of QM are proved to be consistent with the results of these experiments. However, for testing the completeness of QM beyond the electromagnetic interaction regime, it is still a challenge of the test of Bell inequality in high-energy physics (see review Ref. [14] and references therein). At e^+e^- colliders, the testability of BI was first suggested by using the polarization correlation in the process of $e^+e^-\to\Lambda\bar{\Lambda}\to\pi^-p\pi^+\bar{p}$ [15, 16] or $e^+e^-\to Z\to\tau^+\tau^-$ [17−19]. Based on the CHSH method, dedicated proposals were also raised to test BI in the final states of $t\bar{t}$ pair [20−29] or two weak gauge bosons [30−38] at the Large Hadron Collider (LHC). Nevertheless, spin-0 state formed by a pair of spin-1/2 particles in the process such as $e^+e^-\to\Lambda\bar{\Lambda}\to\pi^-p\pi^+\bar{p}$ exhibit the largest entanglement. This is due to the fact that the two spin-1/2 particles emerging from the decay of a spin-0 particle always have the same helicity. Conversely, for the production in a mixture of spin singlet and triplet channels, the magnitude of the correlation is smaller because of the cancellation of different contributions.

The Higgs boson is the only spin-0 elementary particle in the Standard Model (SM) and can play as a natural spin singlet state to test LHVT through the Bell

Received 30 January 2024; Accepted 9 July 2024; Published online 10 July 2024

* Tong Li is Supported by the National Natural Science Foundation of China (12375096, 12035008, 11975129), and "the Fundamental Research Funds for the Central Universities", Nankai University (63196013). Kai Ma was supported by the Natural Science Basic Research Program of Shaanxi Province, China (2023-JC-YB-041) and the Innovation Capability Support Program of Shaanxi Province, China (2021KJXX-47)

† E-mail: makai@ucas.ac.cn
‡ E-mail: litong@nankai.edu.cn (Corresponding author)

inequality at high energies. The properties of SM Higgs boson will be measured to high precision at future e^+e^- colliders such as the Circular Electron Positron Collider (CEPC) [39]. Hence, we propose to test the Bell inequality at CEPC via Higgsstrahlung process with subsequent decay $h\to\tau^+\tau^-$ [27, 40]

$$e^+e^-\to Zh\to Z\tau^+\tau^- . \tag{1}$$

The tau lepton pair is correlated in the decay process, and Bell inequality (or quantum entanglement) can be tested by measuring their spin correlation. However, spin information of the tau leptons can only be partially inferred from its decay particle. Here, we consider only the tau leptons followed by the 1-prong decay mode $\tau^\pm\to\pi^\pm\nu_\tau$ which is the best spin analyzer for the tau lepton polarization. In principle, the other decay modes can also be employed. However, it is more challenging in practice because of the kinematic reconstruction of the tau lepton as well as limited spin analyzing power. To exhibit higher statistics, the associated Z boson will be reconstructed by both its leptonic and hadronic decay modes. Furthermore, Törnqvist's method [15] and CHSH method [4] are explored to evaluate the violation of Bell inequality. To ensure a more realistic estimation on the experimental sensitivities, we investigate the kinematic reconstruction and simulate the detector effects to reveal the quantum entangled spin correlations in the decay of tau pairs.

It should be noted that QM predicts a larger bound of the joint expectation values in CHSH method, i.e., $2\sqrt{2}$ as opposed to 2 [41]. One might suspect that a certain Quantum Mechanics (QM) setup would not violate Bell's inequality. New physics beyond the Standard Model (SM) could potentially alter the angular distributions of tau-lepton decay products. However, there is currently no solid evidence for such new physics, and any deviations from the SM interactions are constrained to be very small. Therefore, our study is conducted based on the assumption that $h\to\tau\tau$ decay and tau decay processes are described by SM.

This study is organized as follows. In Sec. II, we first outline the LHVT and Bell inequality. Then, we show Törnqvist's method and CHSH method in terms of the polarization correlation in decay $h\to\tau^+\tau^-\to\pi^+\bar{\nu}_\tau\pi^-\nu_\tau$. In Sec. III, we describe the simulation of process $e^+e^-\to Zh\to Z\tau^+\tau^-$ and discuss the detector effects as well as reconstruction methods. The results of projected sensitivity to the Bell inequality violation are provided in Sec. IV. Finally, in Sec. V, we summarize our conclusions.

II. LOCAL QUANTUM MODEL AND BELL INEQUALITY

In this section, we describe the original and generalized expressions of Bell inequality and the realistic methods of testing it in high-energy physics.

In the LHVT with the hidden variable being λ, the Bell inequality can be phased in terms of the polarization correlation as follows:

$$P(\vec{a},\vec{b}) = \int \mathrm{d}\lambda\, q(\lambda)\cdot\mathcal{P}_A(\vec{a},\lambda)\cdot\mathcal{P}_B(\vec{b},\lambda), \tag{2}$$

where $\mathcal{P}_{A(B)}(\vec{x},\lambda)$ denotes the probability of the fermion A (or B) with spin along the direction $\vec{x}=\vec{a}\,(\vec{b})$ for a given hidden variable λ, and $q(\lambda)$ is the corresponding probability distribution of the hidden variable λ. The original expression of Bell inequality refers to three independent spatial directions $\vec{a}$, $\vec{b}$, and $\vec{c}$ as:

$$\left|P(\vec{a},\vec{b})-P(\vec{a},\vec{c})\right| \le 1+P(\vec{b},\vec{c}) . \tag{3}$$

On the other hand, in QM, the quantum average of the correlation operator $O(\vec{a},\vec{b}) \equiv \left[\vec{\sigma}^A\cdot\vec{a}\right]\left[\vec{\sigma}^B\cdot\vec{b}\right]$ is given by

$$P(\vec{a},\vec{b}) = \left\langle 00\right|\left[\vec{\sigma}^A\cdot\vec{a}\right]\left[\vec{\sigma}^B\cdot\vec{b}\right]\left|00\right\rangle = -\vec{a}\cdot\vec{b}, \tag{4}$$

where $\langle 00|$ or $|00\rangle$ refers to a singlet state of the total spin. After inserting the QM prediction Eq. (4) in Eq. (3), the Bell inequality Eq. (3) may be violated in some region of phase space. However, in realistic investigations, the spin correlation of the two fermions A and B can only be transferred to the kinematics of their decay products. In terms of $h\to\tau^+\tau^-$ and tau leptons' hadronic decay mode $\tau^\pm\to\pi^\pm\nu_\tau$, we will describe two existing methods to perform the test of Bell inequality at high energy colliders.

A. Törnqvist's method

In Ref. [15], Törnqvist suggested to test the BI by using the polarization correlation in the process:

$$e^+e^-\to\Lambda\bar{\Lambda}\to\pi^- p\pi^+\bar{p} . \tag{5}$$

The parent particle of $\Lambda\bar{\Lambda}$ could be either spin-0 η_c or spin-1 J/ψ. However, instead we established the polarization correlation of decay $h\to\tau^+\tau^-\to\pi^+\bar{\nu}_\tau\pi^-\nu_\tau$. Given that Higgs boson is a scalar and the τ-lepton is a spin-1/2 particle, the decay process $h\to\tau^+\tau^-$ provides an ideal system for testing the Bell inequality. The joint spin density matrix for the $\tau^+\tau^-$ system is as follows:

$$\rho_{\tau\bar{\tau}} = \frac{1}{4}\left(1-\vec{\sigma}_\tau\cdot\vec{\sigma}_{\bar{\tau}}\right), \tag{6}$$

This implies that the state with parallel $\vec{\sigma}_\tau$ and $\vec{\sigma}_{\bar{\tau}}$ van-

ishes because of spin-zero condition. For the correlation operator $O(\vec{a},\vec{b})$, one can easily find the probability as:

$$P(\vec{a},\vec{b}) = \langle 00|\rho_{\tau\bar{\tau}} O(\vec{a},\vec{b})|00\rangle = -\vec{a}\cdot\vec{b}. \tag{7}$$

We show the calculation of the spin correlation coefficients in Appendix A.

However, the spin states of the τ-leptons cannot be measured directly at collider, and they can only be accessed by the angular distributions of their decay products. Here, we only investigate the 1-prong decay mode $\tau^-\to\pi^-\nu_\tau$, in which the momentum direction of the charged pion (or equivlently the neutrino) is correlated to the spin direction of the tau lepton. Thus, this decay mode has the largest spin analyzing power when compared to the cases of the other decay modes. The decay amplitude of process $\tau^-\to\pi^-\nu_\tau$ in the rest frame of the mother particle can be expressed as:

$$\mathcal{M}_\tau = \frac{1}{\sqrt{4\pi}}\left(S + P\vec{\sigma}_\tau\cdot\vec{a}\right), \tag{8}$$

where $\vec{a}$ denotes the unit vector along π^- momentum direction in the rest frame of τ^-, S, and P are S- and P-wave amplitudes, respectively. Similar expression is valid for decay process $\tau^+\to\pi^+\bar{\nu}_\tau$ as well. Then, the probability of π^- flying along $\vec{a}$ and π^+ flying along $\vec{b}$ ($\vec{b}$ is the unit vector along the π^+ momentum direction in the rest frame of τ^+) becomes

$$\begin{aligned}\widetilde{P}(\vec{a},\vec{b}) &= \langle 00|\rho_{\tau\bar{\tau}}\left[\mathcal{M}_\tau\mathcal{M}_{\bar{\tau}}\right]^\dagger\left[\mathcal{M}_\tau\mathcal{M}_{\bar{\tau}}\right]|00\rangle \\ &= \left[\frac{1}{4\pi}\left(|S|^2+|P|^2\right)\right]^2\left(1+\alpha^2\vec{a}\cdot\vec{b}\right),\end{aligned} \tag{9}$$

where

$$\alpha = -\frac{2\Re S P^*}{|S|^2+|P|^2} \approx 0.573. \tag{10}$$

The aforementioned value is obtained by fitting in our numerical simulation. It can be observed that $\widetilde{P}(\vec{a},\vec{b})$ is a partial measurement of the spin states of τ-lepton pair. Its normalized value $\widetilde{P}^N(\vec{a},\vec{b})$ is related to $P(\vec{a},\vec{b})$ by the following relation

$$P(\vec{a},\vec{b}) = \frac{1}{\alpha^2}\left[1-\widetilde{P}^N(\vec{a},\vec{b})\right]. \tag{11}$$

The normalized differential cross section can be expressed as;

$$\frac{1}{\sigma}\frac{\mathrm{d}\sigma}{\mathrm{d}\cos\theta_{ab}} = \frac{1}{2}\widetilde{P}^N(\vec{a},\vec{b}) = \frac{1}{2}\left[1-\alpha^2 P(\vec{a},\vec{b})\right], \tag{12}$$

where $\cos\theta_{ab}\equiv\vec{a}\cdot\vec{b} = -P(\vec{a},\vec{b})$. On the other hand, hidden variable theory predicts [15]:

$$\left|P(\vec{a},\vec{b})\right| \le 1-\frac{2}{\pi}\theta_{ab},\ \ \theta_{ab}\in[0,\pi]. \tag{13}$$

Then, we have the following classical region satisfying the Bell inequality

$$\begin{cases}\dfrac{1}{2}-\alpha^2\left(\dfrac{1}{2}-\dfrac{\theta_{ab}}{\pi}\right)\le\dfrac{1}{\sigma}\dfrac{\mathrm{d}\sigma}{\mathrm{d}\cos\theta_{ab}}\le\dfrac{1}{2}+\alpha^2\left(\dfrac{1}{2}-\dfrac{\theta_{ab}}{\pi}\right), \\ \qquad\theta_{ab}\in[0,\pi/2] \\ \dfrac{1}{2}+\alpha^2\left(\dfrac{1}{2}-\dfrac{\theta_{ab}}{\pi}\right)\le\dfrac{1}{\sigma}\dfrac{\mathrm{d}\sigma}{\mathrm{d}\cos\theta_{ab}}\le\dfrac{1}{2}-\alpha^2\left(\dfrac{1}{2}-\dfrac{\theta_{ab}}{\pi}\right). \\ \qquad\theta_{ab}\in(\pi/2,\pi]\end{cases} \tag{14}$$

B. Clauser-Home-Shimony-Holt inequality

Clauser, Horne, Shimony, and Holt (CHSH) generalized the original Bell inequality Eq. (3) by considering general properties of the quantum density matrix of a spin-1/2 particles system [4]. Density matrix of the quantum state having two spin-1/2 particles can be expressed in general as:

$$\begin{aligned}\rho = \frac{1}{4}\Big[&\mathbb{I}_A\otimes\mathbb{I}_B + A_i\cdot\left(\sigma_{A,i}\otimes\mathbb{I}_B\right) + B_j \\ &\cdot\left(\mathbb{I}_A\otimes\sigma_{B,j}\right) + C_{ij}\left(\sigma_{A,i}\otimes\sigma_{B,j}\right)\Big],\end{aligned} \tag{15}$$

where $\sigma_{A(B),i}$ and $\mathbb{I}_{A(B)}$ are Pauli matrices and unit 2×2 matrix for particle A (B), respectively. The Bell operator associated with the quantum CHSH inequality can be defined as:

$$\mathcal{B}_{\mathrm{CHSH}} = \vec{a}\cdot\vec{\sigma}_A\otimes\left(\vec{b}+\vec{b}'\right)\cdot\vec{\sigma}_B + \vec{a}'\cdot\vec{\sigma}_A\otimes\left(\vec{b}-\vec{b}'\right)\cdot\vec{\sigma}_B, \tag{16}$$

where $\vec{a}$, $\vec{a}'$, $\vec{b}$, $\vec{b}'$ are unit vectors. Then, the CHSH inequality can be provided by [42]

$$\left|\mathrm{Tr}(\rho\mathcal{B}_{\mathrm{CHSH}})\right| \le 2. \tag{17}$$

Similarly, in practice it is hard to test the above inequality directly because of the challenge in measuring of the spin directions $\vec{a}$, $\vec{a}'$, $\vec{b}$, $\vec{b}'$. Alternatively, the matrix with following coefficients

$$C_{ij} = \mathrm{Tr}\left[\rho\sigma_i \otimes \sigma_j\right], \tag{18}$$

can provide an indirect inequality. It is shown that if sum of the two largest eigenvalues of the matrix $U = C^T C$ is larger than 1, then the CHSH inequality is violated [42].

At colliders, the density matrix can be estimated by angular distributions of the two spin-1/2 particles' decay products. The normalized differential cross section can be generally parameterized as [43]:

$$\frac{\sigma^{-1}\mathrm{d}\sigma}{\mathrm{d}\cos\theta_{A,i}\mathrm{d}\cos\theta_{B,j}} = \frac{1}{4}\Big[1 + A_i\cos\theta_{A,i} + B_j\cos\theta_{B,j} + C_{ij}\cos\theta_{A,i}\cos\theta_{B,j}\Big], \tag{19}$$

where $\theta_{A(B),i(j)}$ denote the polar angle of charged particles A (B) from the decays of their mother particles that are measured from $i(j)$-th axis. The helicity basis is always chosen for the spins of the two taus. In our case of $h\to\tau^+\tau^-\to\pi^+\bar{\nu}_\tau\pi^-\nu_\tau$, the cosine quantities of the above polar angles are defined as:

$$\cos\theta_{\pi^+,i} = \hat{p}_{\pi^+}\cdot\hat{i}, \quad \cos\theta_{\pi^-,j} = \hat{p}_{\pi^-}\cdot\hat{j}, \tag{20}$$

where unit vectors $\hat{i}$ and $\hat{j}$ are defined in the rest frames of τ^+ and τ^-, respectively. They belong to a chosen orthonormal basis $\hat{j}\in\{\hat{k},\hat{r},\hat{n}\}$ and satisfy the relation $\hat{i} = -\hat{j}$. More precisely, we define a unit vector $\hat{k}$ as the direction of τ^- momentum in the rest frame of the Higgs boson. In the rest frame of τ^- lepton, we define a unit vector $\hat{r}$ in the decay plane of the τ^- lepton and perpendicular to $\hat{k}$, and a unit vector $\hat{n} = \hat{k}\times\hat{r}$. It was shown that the matrix C can be calculated as [21, 43]:

$$C_{ij} = -9\int \mathrm{d}\cos\theta_{A,i}\mathrm{d}\cos\theta_{B,j}\frac{\sigma^{-1}\mathrm{d}\sigma}{\mathrm{d}\cos\theta_{A,i}\mathrm{d}\cos\theta_{B,j}}\cos\theta_{A,i}\cos\theta_{B,j}. \tag{21}$$

Then, one can diagonalize the spin correlation matrix $C^{\mathrm{T}}C$ and determine the two largest eigenvalues to test the CHSH inequality. Given that the Higgs boson is considered to be on-shell and its spin is zero, there is no invariant mass and orientation dependencies when compared to $t\bar{t}$ final states in Ref. [21].

III. MEASUREMENTS AT FUTURE LEPTON COLLIDERS

At e^+e^- colliders, the dominant production mode of the Higgs boson is the so-called Higgsstrahlung channel, $e^+e^-\to Zh$. For our interested mode $h\to\tau^+\tau^-$ with subsequent decay channels $\tau^\pm\to\pi^\pm\nu$, two neutrinos appear in the final state. Hence, kinematic reconstruction is necessary to measure quantum entanglement between τ^+ and τ^-. Next, we describe our numerical simulation and implementation of the detector effects and then the reconstruction approaches in both the leptonic and hadronic decay modes of Z boson.

A. Simulation and detector effects

Our numerical simulations are conducted using `MadGraph5_aMC@NLO` [44] package, and the quantum entangled spin correlations in the tau-lepton decay are preserved by TauDecay [45] package. For a realistic simulation, detector resolutions have to be included for the objects. Charged tracks can be precisely measured by the CEPC detector for the decay products in $Z\to\ell^+\ell^-$ ($\ell = e,\mu$) or $\tau^\pm\to\pi^\pm\nu$. Table 1 lists typical uncertainties of the azimuthal angle (ϕ), rapidity (η), and magnitude of the transverse momentum ($|\vec{p}_T|$) at CEPC [39]. It can be observed that the CEPC uncertainties for tracks are quite small. We smear tracks (both leptons and pions) by randomly sampling the azimuthal angle, pseudo-rapidity, and transverse momentum according to Gaussian distribution with standard deviations listed in Table 1 [46, 47].

However, the uncertainties associated with jets from Z boson hadronic decays are relatively large. The measurement of jets is not only affected by the fragmentation of partons and the corresponding jet clustering processes, but also by the clustering of reconstructed objects after detector response and their matching to the jets at the generator level [48]. The results in Ref. [49, 50] indicate that the uncertainty induced by the jet clustering and matching can be as significant as those from the detector response, and it becomes the dominant uncertainty especially for final state with more than two jets. Hence, sophisticated jet clustering algorithm has to be used [48]. The energy resolution of the jet from light quarks can be described as [39]:

$$\sigma_{\mathrm{jet}}(E) = \frac{25.7\%}{\sqrt{E}}\oplus 2.4\%. \tag{22}$$

Jets from charm and bottom quarks have slightly larger uncertainties because of neutrinos in their decays [39]. In consideration of this, in this study, we also use a smearing algorithm to account for detector resolutions. Detector responses to the partons (for channel $Z\to q\bar{q}$) are included by smearing energy of the partons according to Gaussian distribution with standard deviations provided

Table 1. CEPC uncertainties for tracks.

Observables	Uncertainties
ϕ	$0.0002\lvert\eta\rvert + 0.000022$
η	$0.000016\lvert\eta\rvert + 0.00000022$
$\lvert\vec{p}_T\rvert$	$0.036\lvert\vec{p}_T\rvert$

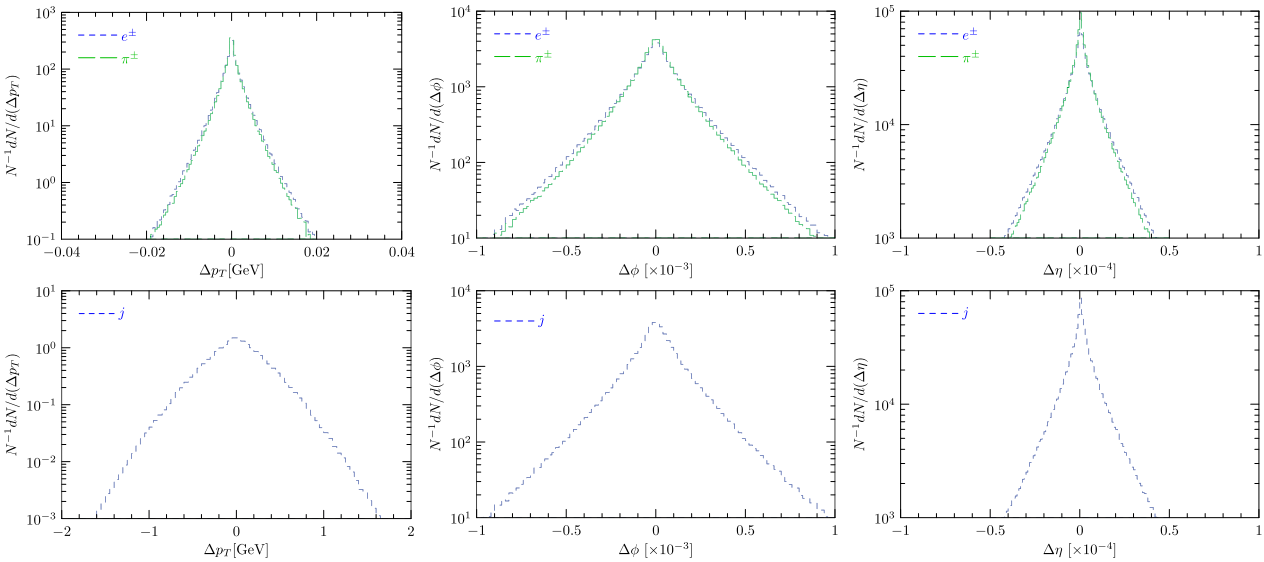

Fig. 1. (color online) Normalized number of events as a function of Δp_T (left), $\Delta\phi$ (middle) and $\Delta\eta$ (right) for the objects (blue: $e^{\pm}$ or jet j, green: $\pi^{\pm}$) in leptonic (top) and hadronic (bottom) decay modes of Z boson.

in Eq. (22).

To observe the impact of the aforementioned uncertainties, in Fig. 1, we show the distributions of the difference between the real value and smeared value of transverse momentum p_T, azimuthal angle ϕ, and rapidity η (defined as Δp_T, $\Delta\phi$ and $\Delta\eta$) for the objects in different decay modes of Z boson. It can be observed that due to the jet energy smearing, the p_T uncertainties of jets in Z boson's hadronic decay are quite large when compared to those in the leptonic mode. Hence, the Z boson decaying to dijet is not well reconstructed as shown in Fig. 2.

Furthermore, detection efficiency is also affected by particle identification. For CEPC, the detector is designed to identify prompt leptons with high efficiency and high purity [39]. For leptons with energies above 5 GeV, the identification efficiency is higher than 99% and misidentification rate is smaller than 2%. For τ-jet with visible energy between 20 and 80 GeV, the identification efficiency exceeds 80% with a purity closing to 90% [39], and further improvement can be expected by optimizations. In our simulation, we ignore the momentum dependence and use an universal identification efficiency 80% estimate experimental significance for τ-jet. For jets from hadronic decay of the Z boson, b-jets can be tagged with an efficiency of 80% and a purity of 90%. Similarly, an efficiency of 60% and a purity of 60% can be realized for the c-jet tagging [39]. In our case, given that the Z boson is treated inclusively, jet-tagging is irrelevant to our analysis. Therefore, we will use an factor of 0.8 to account for possible efficiency loss in reconstruction at the detector level.

B. Reconstruction method

For the decay of the Higgs boson, the corresponding phase space has 8 degrees of freedom, 6 of which can be measured due to the presence of two charged pions. Hence, only 2 degrees of freedom remain undetermined. Considering that the decay width of the τ-lepton is very small compared to its mass, it is a reasonable approximation to assume that both τ-leptons are on-shell. With the aid of the on-shell conditions, all 8 kinematic degrees of freedom can be determined. In the following studies, we always assume that the Z-boson is reconstructed from its visible decay products, and the momentum of the Higgs boson is obtained using the energy-momentum conservation condition, *i.e.*, $p_h = p_{e^+} + p_{e^-} - p_Z$. In the approximation of $P^0 = \sqrt{s}$, and $\vec{P} = 0$ with $P = p_{e^+} + p_{e^-}$, invariant mass of the Higgs momentum is given by $p_h^2 = s + p_Z^2 - 2E_Z\sqrt{s}$. Given that the decay width of Higgs boson is also expected to be very small, $p_h^2 \approx m_h^2$ is again an excellent approximation. In practice, $p_h^2 \equiv \hat{m}_h^2$ may deviate from m_h^2 significantly due to experimental uncertainties in measurement of the Z boson momentum.

Given that the Higgs boson decays isotropically, the reconstruction is done in the rest frame of h. Assuming that both τ-leptons are on-shell, then energy and magnitude of the τ-lepton momentum in this reference frame can be obtained directly as follows:

$$E_\tau^\star = \frac{1}{2}\hat{m}_h, \quad p_\tau^\star = \frac{1}{2}\hat{m}_h\sqrt{1-\frac{4m_\tau^2}{\hat{m}_h^2}}. \tag{23}$$

Intersection angles between momentum of $\tau^\pm$ and $\pi^\pm$ in this frame are as follows:

$$\cos\theta_\pm^\star = \frac{2E_\tau^\star E_{\pi^\pm}^\star - m_\tau^2 - m_{\pi^\pm}^2}{2p_\tau^\star p_{\pi^\pm}^\star}. \tag{24}$$

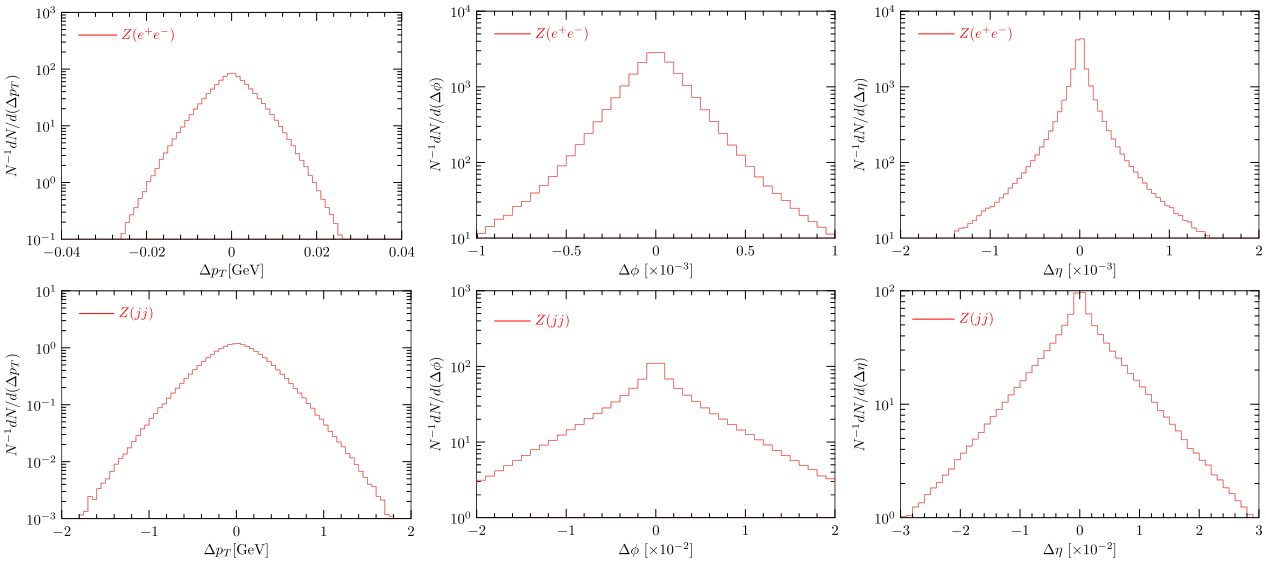

Fig. 2. (color online) Normalized number of events as a function of Δp_T (left), $\Delta\phi$ (middle), and $\Delta\eta$ (right) for the Z boson in leptonic (top) and hadronic (bottom) decay modes.

Without loss of generality, we define z-axis as the momentum direction of the negatively charged decay product, and the positively charged decay product lies in $x-z$ plane. In this reference frame, momenta of the of the charged decay products can be expressed as:

$$p^{\star\mu}_{\pi^-} = E^\star_{\pi^-}\left(1,0,0,\beta^\star_{\pi^-}\right), \tag{25}$$

$$p^{\star\mu}_{\pi^+} = E^\star_{\pi^+}\left(1,\beta^\star_{\pi^+}\sin\theta^\star_{\pi^+},0,\beta^\star_{\pi^+}\cos\theta^\star_{\pi^+}\right). \tag{26}$$

Furthermore, defining the azimuthal angle of τ^--lepton as $\phi^\star_-$, its momentum can be parameterized as:

$$p^{\star\mu}_{\tau^-} = E^\star_\tau\left(1,\beta^\star_\tau\sin\theta^\star_-\cos\phi^\star_-,\beta^\star_\tau\sin\theta^\star_-\sin\phi^\star_-,\beta^\star_\tau\cos\theta^\star_-\right), \tag{27}$$

where $\beta^\star_\tau = \sqrt{1-4m_\tau^2/\hat{m}_h^2}$. It turns out that momentum of τ^+-lepton can be expressed as:

$$p^{\star\mu}_{\tau^+} = E^\star_\tau\left(1,-\beta^\star_\tau\sin\theta^\star_-\cos\phi^\star_-,-\beta^\star_\tau\sin\theta^\star_-\sin\phi^\star_-,-\beta^\star_\tau\cos\theta^\star_-\right). \tag{28}$$

Using equation, $\vec{p}^{\,\star}_{\tau^+}\cdot\vec{p}^{\,\star}_{\pi^+} = \cos\theta^\star_+\left|\vec{p}^{\,\star}_{\tau^+}\right|\left|\vec{p}^{\,\star}_{\pi^+}\right|$, we can immediately express:

$$-\sin\theta^\star_{\pi^+}\sin\theta^\star_-\cos\left(\phi^\star_-\right)-\cos\theta^\star_{\pi^+}\cos\theta^\star_- = \cos\theta^\star_+. \tag{29}$$

Then, we obtain the following solutions,

$$\phi^\star_- = \pm\arccos\left[-\frac{\cos\theta^\star_{\pi^+}\cos\theta^\star_- + \cos\theta^\star_+}{\sin\theta^\star_{\pi^+}\sin\theta^\star_-}\right]. \tag{30}$$

Both solutions satisfy all the kinematic constraints. Hence, there is a two-fold ambiguity.

We then test the above analytical reconstruction method at parton level. Figure 3 shows the longitudinal and transverse correlations as a result of the aforementioned analytical solutions for the leptonic decay mode of Z boson. In the left panel of Fig. 3, the colored densities indicate the true values of $\cos\theta_{\pi^+}$ versus $\cos\theta_{\pi^-}$ and the black contours show the reconstructed values. The above two-fold ambiguity induces a reduction of the transverse spin correction, which is described by the azimuthal angle difference of the two decay planes $\delta\phi$ as shown in the right panel of Fig. 3. In the leptonic decay mode of Z, it can be observed that the aforementioned analytical reconstruction method works well.

However, there are some drawbacks in this analytical reconstruction method. First, the two-fold ambiguity of kinematic solutions exists as mentioned above. One cannot determine the complete $\phi^\star_-$ distribution at a time. More importantly, due to the energy uncertainty of jets, the Z boson cannot be well reconstructed in its hadronic decay mode. Hence, the uncertainties of the Higgs momentum given by analytical reconstruction are very large in the hadronic decay mode of Z boson. Quantum correlation effects are completely washed out, hence it is nearly impossible to observe violation of the Bell identity in the hadronic mode. Therefore, we adopt the other reconstruction method by using impact parameters in next section.

C. Reconstruction by using impact parameters

It is shown that impact parameters of the charged πs

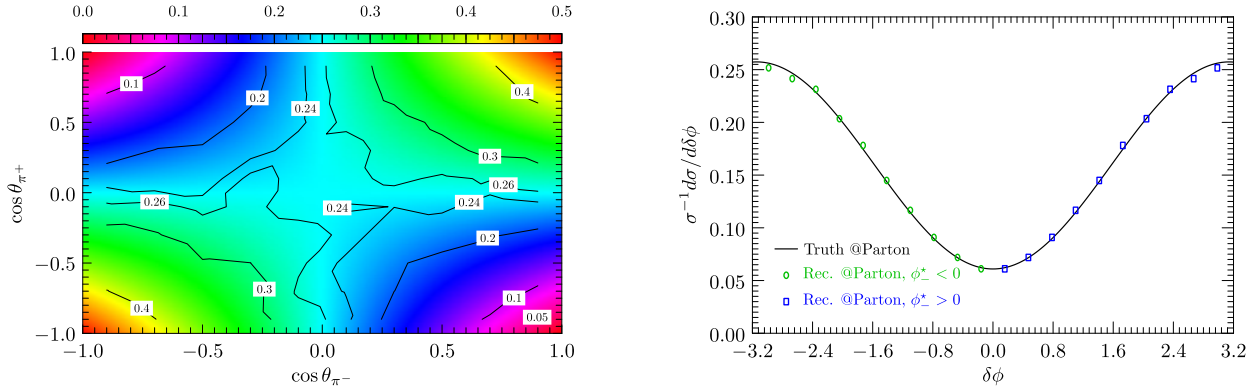

Fig. 3. (color online) Longitudinal (left) and transverse (right) correlations as a result of analytical reconstruction method for leptonic decay mode of Z boson at parton level.

are very useful to reconstruct the full decay kinematics [51−53]. τ-leptons emerging from Higgs decay are strongly boosted. Hence, its typical decay length $\sim 3000\ \mu$m is sufficiently long to induce sizable impact parameter for the charged decay product. The CMS group has used the impact parameter to study CP property of the interaction between Higgs and the tau pair [54]. Here we adopt a similar method proposed in Ref. [51]. Furthermore, excellent impact parameter resolution can be achieved by the CEPC vertex detector. The main performance goals for spatial resolution near the IP can be better than 3 μm [55]. Here, the real impact parameters of the pions are smeared according to Gaussian distribution with standard deviations $\sigma_{\rm IP} = 3\ \mu$m.

We use magnitudes of $\tau^{\pm}$ momenta, $|\vec{p}_{\tau^{\pm}}|$, as the free parameters for finding the best fit. For single tau decay, for instance $\tau^-\to\pi^-\nu_\tau$, the opening angle between τ^- and π^- is:

$$\cos\theta_{\tau^-\pi^-} = \frac{2E_{\tau^-}E_{\pi^-} - m_\tau^2 - m_{\pi^-}^2}{2|\vec{p}_{\tau^-}||\vec{p}_{\pi^-}|}, \tag{31}$$

where $E_{\tau^-} = \sqrt{m_\tau^2 + |\vec{p}_{\tau^-}|^2}$ is given by the on-shell condition. Then, the momentum of τ^- can be expressed as:

$$\vec{p}_{\tau^-} = |\vec{p}_{\tau^-}| \cdot \frac{\vec{b}_{\pi^-} + \dfrac{|\vec{b}_{\pi^-}|}{\tan\theta_{\tau^-\pi^-}} \dfrac{\vec{p}_{\pi^-}}{|\vec{p}_{\pi^-}|}}{\left|\vec{b}_{\pi^-} + \dfrac{|\vec{b}_{\pi^-}|}{\tan\theta_{\tau^-\pi^-}} \dfrac{\vec{p}_{\pi^-}}{|\vec{p}_{\pi^-}|}\right|}, \tag{32}$$

where $\vec{b}_{\pi^-}$ denotes the impact parameter of π^-. Momentum of the neutrino can be obtained by the momentum conservation condition, $p^\mu_{\nu_\tau} = p^\mu_{\tau^-} - p^\mu_{\pi^-}$. Similarly, one can obtain momenta of τ^+ and anti-neutrino as functions of parameter $|\vec{p}_{\tau^+}|$ and impact parameter $\vec{b}_{\pi^+}$. The best values of parameters $|\vec{p}_{\tau^\pm}|$ are obtained by minimizing following likelihood function:

$$L = L_{\rm BW}(\hat{m}_{\tau\tau}, m_Z, \Gamma_Z)\cdot L_{\rm G}(\hat{m}_{\tau\tau} - m_Z, \Gamma_Z) \cdot \prod_{\mu=0,1,2,3} L_{\rm G}(\hat{p}_Z^\mu - p_Z^\mu, \sigma_Z^\mu), \tag{33}$$

where $L_{\rm BW}$ denotes the usual Breit-Wigner distribution for the resonant production of Z boson, and $\hat{m}_{\tau\tau}$ denotes the reconstructed invariant mass of the tau-lepton pair; $\hat{p}_Z^\mu$ denotes the reconstructed momentum of Z boson, and p_Z^μ denotes the momentum obtained by summing momenta of its decay product; $L_{\rm G}(x,y)$ denotes the Gaussian function with mean value x and variance y. Here, σ_Z^μ is estimated by our numerical simulation.

In Figs. 4 and 5, after using the method of impact parameters, we show the observable uncertainties for the reconstructed τ lepton and reconstructed Z mass in different decay modes of Z boson, respectively. It turns out that the reconstruction in hadronic mode is as good as that in leptonic mode for azimuthal angle, rapidity, and the reconstructed Z boson mass. The reconstructed transverse momentum p_T in hadronic mode is still worse than that in leptonic mode. Furthermore, we display the reconstructed longitudinal and transverse correlations for hadronic and leptonic decay modes of Z in Fig. 6. As observed in the bottom panel, the reconstructed transverse correlation is in good agreement with the true result at parton level. It becomes evident that the method of impact parameters does not have the drawback of two-fold ambiguity.

Finally, in Fig. 7, we show the distribution of $\cos\theta_{\pi\pi}$ for hadronic (red) and leptonic (blue) decay modes of Z and compare it with Bell inequality. The LHVT is valid within the two dashed lines (gray fitted region) as defined by the inequality in Eq. (14). The black solid line represents the normalized differential cross section from Eq. (12), with the parton-level results shown as green dots. The simulation results, obtained using the method of impact parameters, are depicted by the red and blue histograms for the hadronic and leptonic decay modes of the Z boson, respectively. A visual inspection of the distributions indicates that they lie outside the region satisfying

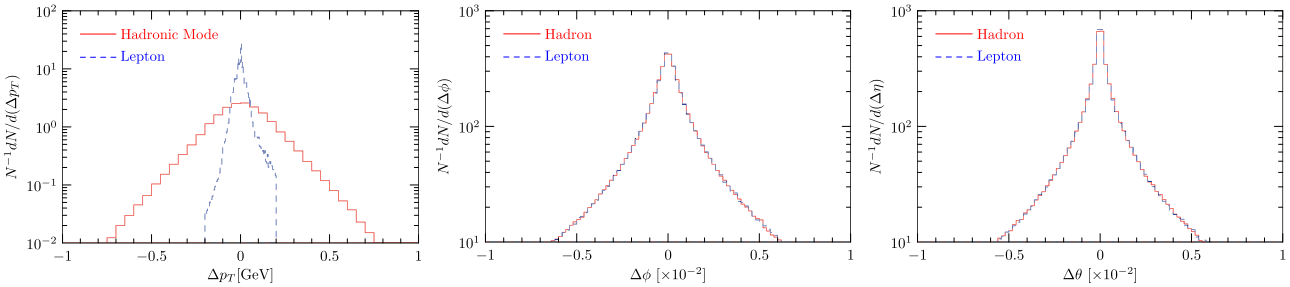

Fig. 4. (color online) Normalized number of events as a function of Δp_T (left), $\Delta\phi$ (middle), and $\Delta\eta$ (right) for the reconstructed τ lepton in leptonic (blue) and hadronic (red) decay modes of Z boson.

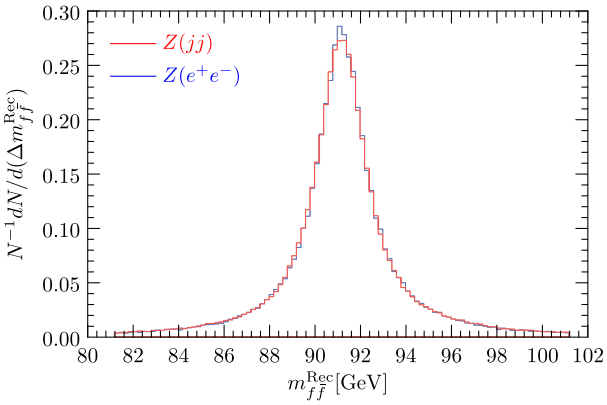

Fig. 5. (color online) Normalized number of events as a function of reconstructed Z mass $m_{f\bar{f}}^{\rm Rec}$ in leptonic (red) and hadronic (blue) decay modes of Z boson.

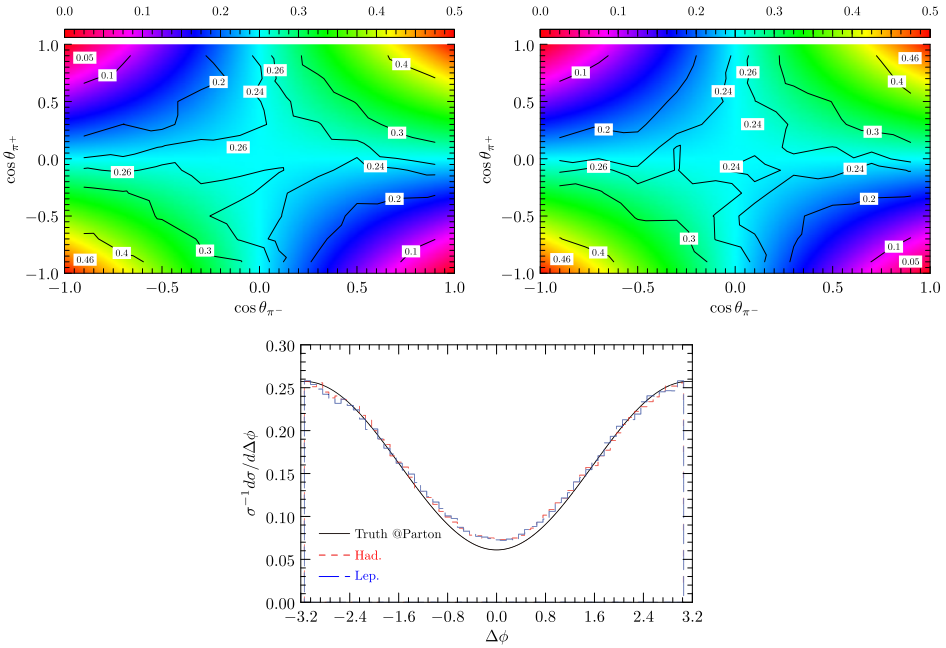

Fig. 6. (color online) Reconstructed longitudinal (top) and transverse (bottom) correlations for hadronic (top left) and leptonic (top right) decay modes of Z boson.

Bell's inequality and align with the QM/QFT prediction shown by the black solid line.

Figure 8 shows the reconstructed angular distributions of the charged pions. In general, quantum entangle-

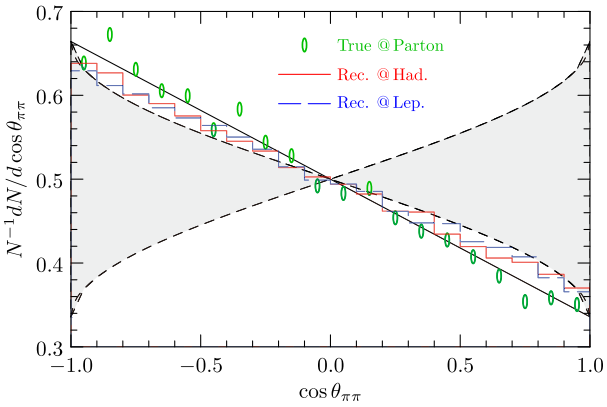

Fig. 7. (color online) Reconstructed distributions of $\cos\theta_{\pi\pi}$ for Törnqvist's test of Bell inequality. The gray-fitted region is the phase space consistent with classical prediction.

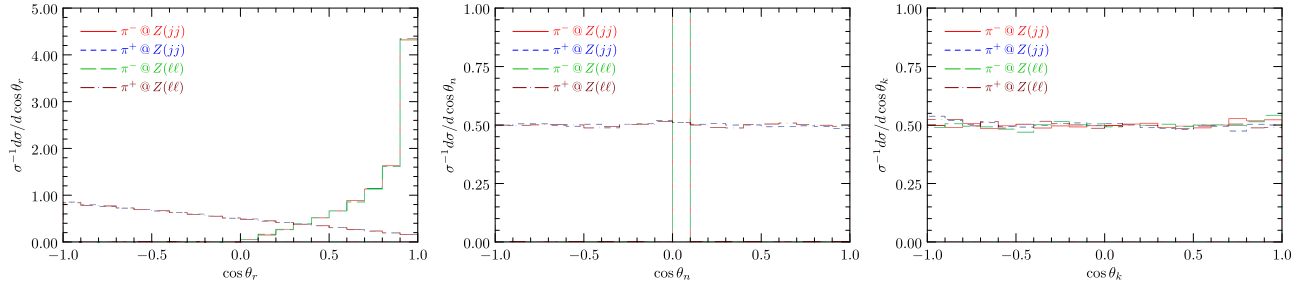

Fig. 8. (color online) Reconstructed angular distributions of $\pi^\pm$ for $\cos\theta_{\pi,r}$ (left), $\cos\theta_{\pi,n}$ (middle), and $\cos\theta_{\pi,k}$ (right).

ment disappears when any single angular observable of the six angles is measured. This is because quantum correlations among π^+ and π^- are integrated out, as shown by the flat distributions in the middle panel for π^+ and right panel for both π^+ and π^-. Given that $x-z$ plane is by definition spanned by the momentum direction of τ^- and π^-, the observable $\cos\theta_{\pi^-,n}$ can only be zero as shown in the middle panel. The nontrivial distributions shown in the left-panel of the Fig. 8 are purely kinematic. Given that $\mathrm{d}\sigma/\mathrm{d}\cos\theta_{\pi^-,k}$ is proportional to a constant and $\theta_{\pi^-,r}=\frac{\pi}{2}-\theta_{\pi^-,k}$, we obtain:

$$\frac{\sigma^{-1}\mathrm{d}\sigma}{\mathrm{d}\cos\theta_{\pi^-,r}}=\frac{\sigma^{-1}\mathrm{d}\sigma}{\mathrm{d}\sin\theta_{\pi^-,k}}\propto \text{const.}\times\cot\theta_{\pi^-,r}\,, \tag{34}$$

which is essentially reconstructed in our approach as shown by the red-solid and green-dashed lines in the left-panel of Fig. 8. Similarly, the asymmetric distribution for π^+ is due to the fact that we defined $\cos\theta_{\pi-,r}>0$, which can lead to a nontrivial integration on the differential cross section $\mathrm{d}\sigma/\mathrm{d}\cos\theta_{\pi-,r}\mathrm{d}\cos\theta_{\pi+,r}\propto 1+C_{rr}\cos\theta_{\pi-,r}\cos\theta_{\pi+,r}$ (the integration region is limited to the range $\cos\theta_{\pi-,r}\in[0,1]$).

It should be noted that calculated coefficients C_{ij} are not really the spin correlation coefficients of the τ-lepton pair. The polar angles in Eq. (19) are defined for πs as opposed to τs. This is a general property of testing Bell-type inequality at colliders because the spin (or helicity state) of the particle under consideration cannot be measured directly. The helicity state can only be inferred partially via the angular distribution of its decay products. For instance, the decay process $\tau\to\pi\nu$ is a good channel to infer the polarization of the mother τ-lepton.

IV. SENSITIVITY OF CEPC TO THE BELL INEQUALITY VIOLATION

In this section, we show the sensitivity of CEPC to the Bell inequality violation. As stated in Sec. III.B, the analytical reconstruction method suffers from the ambiguous two-fold problem. We instead adopt the method of impact parameters for the reconstruction of tau leptons as described in Sec. III.C.

At the CEPC with $\sqrt{s}=240$ GeV, the total cross section of the Higgsstrahlung process is:

$$\sigma_{Zh}=196.2\,\mathrm{fb}\,. \tag{35}$$

A significant number of Higgs boson events will be produced with an expected integrated luminosity of $\mathcal{L}=5.6\,\mathrm{ab}^{-1}$ [39]. However, given that both the branching ratios $\mathcal{B}(h\to\tau\tau)=6.32\%$ and $\mathcal{B}(\tau\to\pi\nu_\tau)=10.82\%$ are small, only hundreds of events are available to test the

Bell inequality. The following kinematic cuts are used to select well-reconstructed events, and match to the real detector configuration:

$$p_T(\ell/j) > 10\,\text{GeV},\ |\eta(\ell/j)| < 3,\ \left|m_{ff}^{\text{Rec.}} - m_Z\right| < 10\,\text{GeV}. \tag{36}$$

The efficiency for the aforementioned kinematic cuts is 0.645 for the decay mode $Z\to\ell\ell$, and 0.648 for the hadronic decay mode $Z\to jj$. Furthermore, as we have mentioned, a universal jet reconstruction efficiency 0.8 will be used in our following estimation. The number of events can be further reduced by τ-jet identification, which is assumed to be 0.8 for a purity closing to 90% at the CEPC [39]. Table 2 lists the expected number of events at the CEPC.

The experimental sensitivity for the Törnqvist's approach is examined by defining the following asymmetric observable:

$$\mathcal{A} = \frac{N(\cos\theta_{\pi\pi} < 0) - N(\cos\theta_{\pi\pi} > 0)}{N(\cos\theta_{\pi\pi} < 0) + N(\cos\theta_{\pi\pi} > 0)}. \tag{37}$$

The analytical prediction of the observable provides an upper bound $\mathcal{A} = 0.119$ in LHVT. The experimental sensitivity at the CEPC is estimated by conducting 10,000 pseudo-experiments, in which as many events as possible are generated to predict the central values and corresponding uncertainties. These uncertainties are then scaled to match the corresponding luminosities. We obtain $\mathcal{A} = 0.133 \pm 0.269$ for $Z\to\ell\ell$ channel and $\mathcal{A} = 0.137 \pm 0.1$ for $Z\to jj$ channel, respectively, as listed in Table 3. Smaller uncertainties can be obtained with $\mathcal{A} = 0.133 \pm 0.142$ or $\mathcal{A} = 0.137 \pm 0.053$ for updated luminosity $\mathcal{L} = 20\ \text{ab}^{-1}$. Both central values are above the bound in LHVT. The channel from the hadronic decay mode of Z boson produces more events and provides more reasonable result with small error. In the CHSH approach, the LHVT supports the fact that the sum of the two largest eigenvalues of the matrix $U = C^T C$ (denoted by $m_1 + m_2$) is not larger than 1. It becomes evident that both channels lead to $m_1 + m_2 > 1$, as listed in Table 3. It can be observed that for Törnqvist's method and CHSH approach, the Bell inequality can only be tested below 1σ level at the CEPC. It is expected that the sensitivity can be further improved by using sophisticated jet reconstruction method and enhanced τ-jet identification efficiency. It should be noted that the results in the fourth and fifth columns of Table 3 are from our detector-level simulation. The simulation results of SM expectation change from parton-level to detector-level. The parton-level and detector-level predictions differ because the experimental uncertainties can diminish the magnitudes of the spin correlation effects as a result of imperfect reconstruction (and also reconstruction efficiency). In this study, we compare the detector-level QM simulation results with the bound in LHVT directly. We will leave the study of a more reasonable comparison in a future study.

It is worth indicating that when compared to the Törnquivst's method, the calculation of the sum of two largest eigenvalues of $C^T C$ as an estimator in the CHSH approach requires the estimation of the spin projections along all the three possible independent directions. Hence, it is relatively more difficult for small data sample. For Törnquivst's method, the bounds provided by Bell inequality on the LHVT are shown by dashed lines in the distribution of $\cos\theta_{\pi\pi}$ in Fig. 7. To provide a quantitative determination of the Bell inequality violation, we define the aforementioned asymmetric observable $\mathcal{A}$. In this manner, the LHVT has a quantitative upper bound as shown in Table 3. Different (quantum) models lead to different values of $\mathcal{A}$ and $m_1 + m_2$, and they are certainly affected by new physics. As stated in Introduction, it is reasonable to assume that $h\to\tau\tau$ decay and tau decay processes are described by the SM. Furtherore, QM prediction in Table 3 is obtained in the SM. Hence, we can claim that the Bell inequality can be tested under the assumption of SM below 1σ level at the CEPC.

In summary, the QM prediction in Table 3 is provided by the parton-level events. The experimental values are based on our Monte-Carlo simulation. There are two

Table 2. Number of events used to test the Bell inequality at the CEPC.

CEPC (240 GeV, 5.6ab^{-1})	$Z\to\ell\ell$	$Z\to jj$
No. of Events	55	568
Kin. Cuts and jet reconstruction	22	151
τ-identification	14	97

Table 3. Results of observables testing Bell inequality in Törnqvist's method and CHSH approach. The experimental predictions are provided for the CEPC with colliding energy $\sqrt{s} = 240\,\text{GeV}$ and total luminosities 5.6 ab^{-1} and 20 ab^{-1}.

Channels	Obs.	Clas.	Exp. @ 5.6 ab^{-1}	Exp. @ 20 ab^{-1}
$Z\to\ell\ell$	$\mathcal{A}$	≤ 0.119	0.133 ± 0.269	0.133 ± 0.142
	$m_1 + m_2$	≤ 1	1.04 ± 0.921	1.04 ± 0.481
$Z\to jj$	$\mathcal{A}$	≤ 0.119	0.137 ± 0.1	0.137 ± 0.053
	$m_1 + m_2$	≤ 1	1.05 ± 0.355	1.05 ± 0.188

factors affecting the disagreement. One is the experimental uncertainty due to the detector effects, which can reduce the quantum correlation such that the result tends to deviate from the QM prediction. The second factor is the reconstruction method. The correlation cannot be reconstructed precisely. Even if the number of events is increased, the deviation still exists.

V. DISCUSSIONS AND CONCLUSIONS

Given that spin state cannot be directly measured at collider, it is a challenge for the test of quantum entanglement and Bell-nonlocality in high-energy collider physics. However, testing Bell-nonlocality in high energy scattering process is essentially important because it provides a unique way to address the quantum entanglement at high energy scale. We investigate the testability of Bell inequality through $h\to\tau^+\tau^-$, which is an ideal system to observe the LHVT violation, at future e^+e^- collider CEPC. We demonstrated how angular distributions of the decay products of spin-correlated τ-pairs can be used to address Bell nonlocality. Future e^+e^- colliders can improve the measurement accuracy of the spin correlation of tau lepton pairs from Higgs boson decay. Two realistic methods of testing Bell inequality, i.e., Törnqvist's method and CHSH inequality are examined in terms of the polarization correlation in decay $h\to\tau^+\tau^-\to\pi^+\bar{\nu}_\tau\pi^-\nu_\tau$.

We simulate the production of $e^+e^-\to Zh\to Z\tau^+\tau^-$ as well as the Z boson's leptonic and hadronic decay modes. The detector effects of CEPC including uncertainties for tracks and jets from Z boson are considered. Furthermore, we describe necessary reconstruction approaches to measure quantum entanglement between τ^+ and τ^-. Finally, we observe that for Törnqvist's method and CHSH approach, the Bell inequality can be tested at the CEPC below 1σ level. Further improvements are expected by employing sophisticated jet reconstruction method and enhanced τ-jet identification efficiency.

We also noted in Ref. [40] that the authors examined the same topic at ILC and FCC-ee. The expected total number of events is 385 at ILC (250 GeV, $\mathcal{L}=3\ \text{ab}^{-1}$) or 663 at FCC-ee (240 GeV, $\mathcal{L}=5\ \text{ab}^{-1}$). Conversely, our estimation for CEPC (240 GeV, $\mathcal{L}=5.6\ \text{ab}^{-1}$) is 111. Even if the total cross section at ILC or FCC-ee is slightly larger (240.1 fb or 240.3 fb) than the one (196.2 fb) at the CEPC, it is too small to have more than 2 times or 5 times larger number of events. Such a difference can only come from the detector effects. The reconstruction of mode $e^+e^-\to Z(\to jj)h(\to\tau_\pi\tau_\pi)$, which has the largest production rate, is rather difficult and thus influences the detector effects on the reconstruction. Given that the jets (from Z or h) are relatively soft at the CEPC (and ILC-250), the usual jet clustering does not lead to appropriate output. Hence, the reconstruction efficiency is rather low. Some sophisticated clustering method should be employed. In our study, we chose the smearing method for CEPC to solve this problem.

Additionally, we proposed to use Törnqvist's method to test the Bell inequality at CEPC. The reason is twofold. First, it is much simpler and more straightforward. Second, in case of the (very) small number of events, the estimation of the correlation efficiency C_{ij} via the integration of the phase space is unstable/unsafe. Hence, this induces a very large fluctuation of the central/expected value of the observable. This can be observed in Table 3, particularly for the leptonic decay mode of Z boson.

ACKNOWLEDGEMENTS

T.L. would like to thank Xue-Qian Li for helpful discussion.

APPENDIX A: SPIN CORRELATION COEFFICIENTS IN TÖRNQVIST'S METHOD

For Törnqvist's method, we calculate the correlation coefficients in the following manner. Assuming τ and $\bar{\tau}$ are polarized along $\vec{a}$ and $\vec{b}$, respectively, their helicity basis can be chosen to be the eigenstates of the helicity opeators $\vec{a}\cdot\vec{\sigma}_\tau$ and $\vec{b}\cdot\vec{\sigma}_{\bar{\tau}}$, respectively. Then, the expected value of the correlation matrix $O(\vec{a},\vec{b})=\left(\vec{a}\cdot\vec{\sigma}_\tau\right)\left(\vec{b}\cdot\vec{\sigma}_{\bar{\tau}}\right)$ can be expressed as:

$$\begin{aligned}&\langle h_\tau h_{\bar{\tau}}|\rho_{\tau\bar{\tau}}O(\vec{a},\vec{b})|h_\tau h_{\bar{\tau}}\rangle\\&=\langle h_\tau h_{\bar{\tau}}|\frac{1}{4}\left(1-\vec{\sigma}_\tau\cdot\vec{\sigma}_{\bar{\tau}}\right)\left(\vec{a}\cdot\vec{\sigma}_\tau\right)\left(\vec{b}\cdot\vec{\sigma}_{\bar{\tau}}\right)|h_\tau h_{\bar{\tau}}\rangle,\end{aligned}\tag{A1}$$

where $h_{\tau(\bar{\tau})}$ denotes the helicity of $\tau(\bar{\tau})$. By using the following relation

$$\vec{\sigma}_\tau\cdot\vec{\sigma}_{\bar{\tau}}=\frac{1}{2}\left(\vec{\Sigma}^2-6\right),\tag{A2}$$

where $\vec{\Sigma}=\vec{\sigma}_\tau+\vec{\sigma}_{\bar{\tau}}$ and $\vec{\Sigma}^2=0$ for spin singlet, we have:

$$\langle h_\tau h_{\bar{\tau}}|\rho_{\tau\bar{\tau}}O(\vec{a},\vec{b})|h_\tau h_{\bar{\tau}}\rangle=\langle h_\tau h_{\bar{\tau}}|\left(\vec{a}\cdot\vec{\sigma}_\tau\right)\left(\vec{b}\cdot\vec{\sigma}_{\bar{\tau}}\right)|h_\tau h_{\bar{\tau}}\rangle=h_\tau h_{\bar{\tau}}.\tag{A3}$$

For $\vec{a}=\hat{e}_z$ and $\vec{b}=\hat{e}_z$, the spin singlet requires the helicities of τ and $\bar{\tau}$ satisfy:

$$h=h_\tau+h_{\bar{\tau}}=0.\tag{A4}$$

Hence, we obtain the correlation coefficients as:

$$C_{zz} = \langle h_\tau h_{\bar\tau}|\rho_{\tau\bar\tau} O(\hat{\vec{e}}_z, -\hat{\vec{e}}_z)|h_\tau h_{\bar\tau}\rangle = h_\tau h_{\bar\tau} = -1\,, \tag{A5}$$

and similarly

$$C_{xx} = \langle h_\tau h_{\bar\tau}|\rho_{\tau\bar\tau} O(\hat{\vec{e}}_x, -\hat{\vec{e}}_x)|h_\tau h_{\bar\tau}\rangle = -1\,,$$
$$C_{yy} = \langle h_\tau h_{\bar\tau}|\rho_{\tau\bar\tau} O(\hat{\vec{e}}_y, -\hat{\vec{e}}_y)|h_\tau h_{\bar\tau}\rangle = -1\,. \tag{A6}$$

The aforementioned calculations show that the correlation coefficients in our helicity basis are $(-1, -1, -1)$. In the above calculations, the condition $\vec{\Sigma}^2 = 0$, which implies $\tau\bar\tau$ system is a spin-singlet, is crucial. Hence, different results may be obtained if the spin projection axis is defined differently.

References

[1] Albert Einstein, Boris Podolsky, and Nathan Rosen, Phys. Rev. **47**, 777 (1935)
[2] D. Bohm and Y. Aharonov, Phys. Rev. **108**, 1070 (1957)
[3] J. S. Bell, Physics Physique Fizika **1**, 195 (1964)
[4] John F. Clauser, Michael A. Horne, Abner Shimony *et al.*, Phys. Rev. Lett. **23**, 880 (1969)
[5] R. A. Bertlmann, Lect. Notes Phys. **689**, 1 (2006), arXiv:quant-ph/0410028
[6] Alain Aspect, Philippe Grangier, and Gerard Roger, Phys. Rev. Lett. **49**, 91 (1982)
[7] Alain Aspect, Jean Dalibard, and Gerard Roger, Phys. Rev. Lett. **49**, 1804 (1982)
[8] Z. Y. Ou and L. Mandel, Phys. Rev. Lett. **61**, 50 (1988)
[9] Gregor Weihs, Thomas Jennewein, Christoph Simon *et al.*, Phys. Rev. Lett. **81**, 5039 (1998), arXiv:quant-ph/9810080
[10] Dik Bouwmeester, Jian-Wei Pan, Matthew Daniell *et al.*, Phys. Rev. Lett. **82**, 1345 (1999), arXiv:quant-ph/9810035
[11] J. W. Pan, D. Bouwmeester, M. Daniell *et al.*, Nature **403**, 515 (2000)
[12] Andrew G. White, Daniel F. V. James, Philippe H. Eberhard *et al.*, Phys. Rev. Lett. **83**, 3103 (1999)
[13] Tao Yang, Qiang Zhang, Jun Zhang *et al.*, Phys. Rev. Lett. **95**, 240406 (2005)
[14] Yi-Bing Ding, Jun-li Li, and Cong-Feng Qiao, *Bell Inequalities in High Energy Physics*, (2007), arXiv:hep-ph/0702271
[15] Nils A. Tornqvist, Found. Phys. **11**, 171 (1981)
[16] Xi-Qing Hao, Hong-Wei Ke, Yi-Bing Ding *et al.*, Chin. Phys. C **34**, 311 (2010), arXiv:0904.1000[hep-ph]
[17] Paolo Privitera, Phys. Lett. B **275**, 172 (1992)
[18] S. A. Abel, M. Dittmar, and Herbert K. Dreiner, Phys. Lett. B **280**, 304 (1992)
[19] Herbert K. Dreiner, *Bell's inequality and tau physics at LEP*, in 2nd Workshop on Tau Lepton Physics, (1992), arXiv:hep-ph/9211203
[20] Yoav Afik and Juan Ramón Muñoz de Nova, Eur. Phys. J. Plus **136**, 907 (2021), arXiv:2003.02280[quant-ph]
[21] M. Fabbrichesi, R. Floreanini, and G. Panizzo, Phys. Rev. Lett. **127**, 161801 (2021), arXiv:2102.11883[hep-ph]
[22] Claudio Severi, Cristian Degli Esposti Boschi, Fabio Maltoni *et al.*, Eur. Phys. J. C **82**, 285 (2022), arXiv:2110.10112[hep-ph]
[23] Yoav Afik and Juan Ramón Muñoz de Nova, Quantum **6**, 820 (2022), arXiv:2203.05582[quant-ph]
[24] J. A. Aguilar-Saavedra and J. A. Casas, Eur. Phys. J. C **82**, 666 (2022), arXiv:2205.00542[hep-ph]
[25] Yoav Afik and Juan Ramón Muñoz de Nova, Phys. Rev. Lett. **130**, 221801 (2023), arXiv:2209.03969[quant-ph]
[26] Rafael Aoude, Eric Madge, Fabio Maltoni *et al.*, Phys. Rev. D **106**, 055007 (2022), arXiv:2203.05619[hep-ph]
[27] Marco Fabbrichesi, Roberto Floreanini, and Emidio Gabrielli, Eur. Phys. J. C **83**, 162 (2023), arXiv:2208.11723[hep-ph]
[28] Mira Varma and O. K. Baker, *Quantum Entanglement in Top Quark Pair Production*, (2023), arXiv:2306.07788[hep-ph]
[29] Zhongtian Dong, Dorival Gonçalves, Kyoungchul Kong *et al.*, *When the Machine Chimes the Bell: Entanglement and Bell Inequalities with Boosted $t\bar{t}$*, (2023), arXiv:2305.07075[hep-ph]
[30] Alan J. Barr, Phys. Lett. B **825**, 136866 (2022), arXiv:2106.01377[hep-ph]
[31] Alan J. Barr, Pawel Caban, and Jakub Rembieliski, *Bell-type inequalities for systems of relativistic vector bosons*, (2022), arXiv:2204.11063[quant-ph]
[32] J. A. Aguilar-Saavedra, Phys. Rev. D **107**, 076016 (2023), arXiv:2209.14033[hep-ph]
[33] J. A. Aguilar-Saavedra, A. Bernal, J. A. Casas *et al.*, Phys. Rev. D **107**, 016012 (2023), arXiv:2209.13441[hep-ph]
[34] M. Fabbrichesi, R. Floreanini, E. Gabrielli *et al.*, *Bell inequalities and quantum entanglement in weak gauge bosons production at the LHC and future colliders*, (2023), arXiv:2302.00683[hep-ph]
[35] Rafael Aoude, Eric Madge, Fabio Maltoni *et al.*, *Probing new physics through entanglement in diboson production*, (2023), arXiv:2307.09675[hep-ph]
[36] Alexander Bernal, Paweł Caban, and Jakub Rembieliński, *Entanglement and Bell inequalities violation in $H \to ZZ$ with anomalous coupling*, (2023), arXiv:2307.13496[hep-ph]
[37] Federica Fabbri, James Howarth, and Theo Maurin, *Isolating semi-leptonic $H \to WW^*$ decays for Bell inequality tests*, (2023), arXiv:2307.13783[hep-ph]
[38] Qi Bi, Qing-Hong Cao, Kun Cheng *et al.*, *New observables for testing Bell inequalities in W boson pair production*, (2023), arXiv:2307.14895[hep-ph]
[39] Mingyi Dong *et al.* (CEPC Study Group), *CEPC Conceptual Design Report: Volume 2 - Physics & Detector*, (2018), arXiv:1811.10545[hep-ex]
[40] Mohammad Mahdi Altakach, Priyanka Lamba, Fabio Maltoni *et al.*, Phys. Rev. D **107**, 093002 (2023), arXiv:2211.10513[hep-ph]
[41] B. S. Cirelson, Lett. Math. Phys. **4**, 93 (1980)
[42] R. Horodecki, P. Horodecki, and M. Horodecki, Phys. Lett. A **200**, 340 (1995)
[43] Werner Bernreuther, Dennis Heisler, and Zong-Guo Si, JHEP **12**, 026 (2015), arXiv:1508.05271[hep-ph]
[44] J. Alwall, R. Frederix, S. Frixione *et al.*, JHEP **07**, 079

(2014), arXiv:1405.0301[hep-ph]
[45] Kaoru Hagiwara, Tong Li, Kentarou Mawatari *et al*., Eur. Phys. J. C **73**, 2489 (2013), arXiv:1212.6247[hep-ph]
[46] J. de Favereau, C. Delaere, P. Demin *et al*. (DELPHES 3), JHEP **02**, 057 (2014), arXiv:1307.6346[hep-ex]
[47] Toshinori Abe *et al*. (Linear Collider ILD Concept Group), *The International Large Detector: Letter of Intent*, (2010), arXiv:1006.3396[hep-ex]
[48] Manqi Ruan *et al*., Eur. Phys. J. C **78**, 426 (2018), arXiv:1806.04879[hep-ex]
[49] Pei-Zhu Lai, *Jet Reconstruction at the CEPC (2017)*, CEPC-REC-2017-002
[50] Pei-Zhu Lai, Manqi Ruan, and Chia-Ming Kuo, JINST **16**, P07037 (2021), arXiv:2104.05029[hep-ex]
[51] Kaoru Hagiwara, Kai Ma, and Shingo Mori, Phys. Rev. Lett. **118**, 171802 (2017), arXiv:1609.00943[hep-ph]
[52] D. Jeans and G. W. Wilson, Phys. Rev. D **98**, 013007 (2018), arXiv:1804.01241[hep-ex]
[53] Xin Chen and Yongcheng Wu, Phys. Lett. B **790**, 332 (2019), arXiv:1708.02882[hep-ph]
[54] Armen Tumasyan *et al*. (CMS), JHEP **06**, 012 (2022), arXiv:2110.04836[hep-ex]
[55] Muhammd Ahmad *et al*., *CEPC-SPPC Preliminary Conceptual Design Report. 1. Physics and Detector*, (2015)